Simon Binder, Adrian Ehrenhofer, Tanvir Ahmad, Christopher F. Reiche, Florian Solzbacher, Thomas Wallmersperger

# Localized actuation of temperature responsive hydrogel-layers with a PCB-based micro-heater array

**Erstveröffentlichung in / First published in:**

*SPIE Smart Structures + Nondestructive Evaluation.* Long Beach, 0603.–11.04.2021. Bellingham: SPIE, Vol. 12042 [Zugriff am: 26.05.2022].

DOI: https://doi.org/10.1117/12.2612335

# Localized actuation of temperature responsive hydrogel-layers with a PCB-based micro-heater array

Binder, Simon, Ehrenhofer, Adrian, Ahmad, Tanvir, Reiche, Christopher, Solzbacher, Florian, et al.

Simon Binder, Adrian Ehrenhofer, Tanvir Ahmad, Christopher F. Reiche, Florian Solzbacher, Thomas Wallmersperger, "Localized actuation of temperature responsive hydrogel-layers with a PCB-based micro-heater array," Proc. SPIE 12042, Electroactive Polymer Actuators and Devices (EAPAD) XXIV, 120420S (20 April 2022); doi: 10.1117/12.2612335

SPIE.

Event: SPIE Smart Structures + Nondestructive Evaluation, 2022, Long Beach, California, United States

# Localized actuation of temperature responsive hydrogel-layers with a PCB-based micro-heater array

Simon Binder[a], Adrian Ehrenhofer[b, c], Tanvir Ahmad[a], Christopher F Reiche[a], Florian Solzbacher[a], and Thomas Wallmersperger[c, b]

[a]Department of Electrical and Computer Engineering, University of Utah, Salt Lake City, UT, 84112 USA

[b]Dresden Center for Intelligent Materials, Technische Universität Dresden, 01062 Dresden, Germany

[c]Institute of Solid Mechanics, Technische Universität Dresden, 01062 Dresden, Germany

## ABSTRACT

The space-resolved manipulation of a surface can be achieved by triggering a temperature induced swelling response locally by using a micro-heater array. In this work, we present the interaction of (i) a rigid array of heating elements that can be selectively activated and (ii) thermo-responsive hydrogel pillars that respond to the local stimulus change. The heating elements are Platinum wire heaters, which are fabricated via surface micromachining techniques on a printed circuit board (PCB). A polyimide thin film is used as a thin membrane beneath the micro heaters and as a protective encapsulation on top of the micro-heaters. The heaters are arranged in a 10 by 10 array and occupy an area of 15 mm x 15 mm. The UV-structured smart hydrogel layer is made of poly(N-isopropyl-acrylamide) with Lower Critical Solution Temperature (LCST) behavior. The setup features single pillars with a diameter of 750 µm on each single microheater. The design of the system is based on continuum-based simulations using the Temperature Expansion Model in the framework of the Finite-Element tool Abaqus. Based on the simulations, the system's capability for micro-manipulation is assessed. The analysis of the described system offers further insights into the behavior of locally actuated active polymers and their interaction with rigid systems.

**Keywords:** Micromanipulation platform, hydrogels, microheaters, hydrogel-based actuator

## 1. INTRODUCTION TO MICROMANIPULATION PLATFORMS

Spatially resolved manipulation of surfaces is part of numerous applications. In this case spatially resolved surface manipulation means locally lowering or raising a surface, so that curvatures or inclinations of the surface are caused. Exemplary applications are micromechanical mirrors,[1,2] adaptive lenses[3] or tactile[4] and Braille displays.[5] The actuator principles used for such applications are manifold and involve, for example, piezoelectric,[6] electromagnetic,[7] electrostatic[7] or pneumatic[8] actuators as well as actuators based on electroactive polymers such as dielectric elastomer actuators,[9,10] electrostrictive polymers,[11] shape memory alloys[12] or thermo-pneumatic actuators.[13,14] Particularly for adaptive lenses, electrowetting[15] or micropneumatic actuators[16] are used.

While many of the actuator principles mentioned above are not designed for aqueous environments or require sealing when operating in water, an alternative actuator principle - the hydrogel-based actuator - on the contrary even requires an aqueous environment. A hydrogel actuator's operating principle is based particularly on the absorption and release of water, which is why it is virtually predestined for application in aqueous environments. An additional advantage of hydrogel actuators is their comparatively high energy density.[17] At the same time, these actuators are easy to miniaturize and can be fabricated using manufacturing processes similar to those used for MEMS devices. Hydrogel-based actuators have already been applied in the past for various actuating tasks

Further author information:
Simon Binder: E-mail: simon.binder@utah.edu
Adrian Ehrenhofer: E-mail: adrian.ehrenhofer@tu-dresden.de
Simon Binder and Adrian Ehrenhofer contributed equally.

Electroactive Polymer Actuators and Devices (EAPAD) XXIV, edited by Iain A. Anderson
John D. W. Madden, Herbert R. Shea, Proc. of SPIE Vol. 12042, 120420S
© 2022 SPIE · 0277-786X · doi: 10.1117/12.2612335

like microvalves,[18] micropumps,[19] particle filters,[20] compensated sensors[21] or tactile displays.[4] Thermoresponsive hydrogels in particular are the preferred choice for these applications because they can be easily controlled by means of small heating elements.[19]

The functional principle of thermoresponsive hydrogel actuators is based on the lower critical solution temperature behavior (LCST) of the polymer used for the hydrogel. In the hydrophilic polymer network, this property leads to a temperature-dependent water uptake of the hydrogel. When passing through the associated volume phase transition, the hydrogel can perform mechanical work. A hydrogel often used for this purpose is based on the polymer *net*-PNiPAAm which has an LCST of approx. 32 °C.[22]

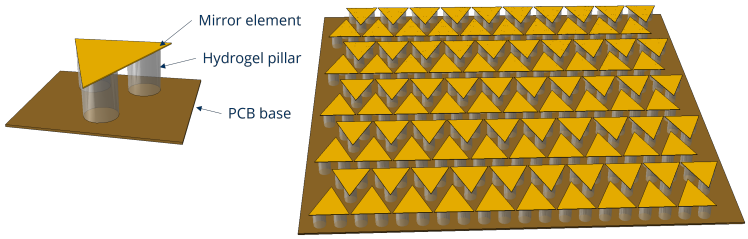


Figure 1: The microheater array is intended to carry an array of mirror elements that are manipulated by the localized heating of hydrogel pillars mounted on a printed circuit board (PCB) substrate that contains a microheater array.

In this work, we selectively excite a *net*-PNiPAAm-based hydrogel actuator array by means of separate microheaters, see Figure 1. To achieve such a hydrogel actuator array with individually controllable microheaters, a recently developed method for fabricating low-power membrane-mounted microheaters is used.[23] The aim of the current work is to theoretically examine and experimentally test this microheater array in combination with temperature-responsive hydrogel actuators with the intention to locally lower or raise a surface in an aqueous environment. Thermal actuation of the hydrogel actuators is accomplished using a 10x10 array of microheaters distributed over an area of approx. 15 x 15 $mm^2$. The microheaters are created on a polyimide membrane using microfabrication techniques. A printed circuit board (PCB) serves as the substrate for the hydrogel-based surface micromanipulation platform.

The present paper is structured as follows: The thermo-responsive hydrogel and the microheater array fabrication are described in section 2. This is followed by the description of modeling and simulation of these kinds of structures in section 3. Swelling and simulation results are shown in section 4. The conclusion and outlook is drawn in section 5.

## 2. ACTIVE HYDROGEL LAYER WITH A MICROHEATER ARRAY AS ACTUATING PLATFORM

In the current section, the fabrication of the microheater array (section 2.1) and the hydrogels (section 2.2) is presented. Subsequently, the design of the free swelling experiments (section 4.1) and the pillar actuation (section 2.4) are described.

### 2.1 Microheater array

A similar fabrication method for a 10x10 array of polyimide membrane-suspended microheaters has been presented previously.[23] Process parameter details are given there. The membrane diameter in the current work was increased from 500 µm to 750 µm. Essential manufacturing steps are given as follows, with Figure 2 illustrating these process steps.

A PCB with the dimensions 26 mm x 26 mm x 1.2 mm (PCBway) was used as substrate. The PCB has 10x10 holes with diameters of 750 µm at regular intervals and 200 copper vias with diameters of 500 µm each for later contacting of the microheaters, see Figure 2 a. A thin polyimide film (Kapton 150FN019, 25.4 µm thickness with 12.7 µm thick adhesive layer, Dupont) is laminated onto this PCB using a heat press. As a result, thin membranes with a diameter of 750 µm are formed over the recesses of the PCB, see Figure 2 b. To remove the polyimide,

which is covering the copper vias, a modified encapsulation layer opening technique using laser ablation was used (see Figure 2 c). Subsequently, the meander-shaped platinum microheater structures are sputter-deposited on the polyimide, see Figure 2 d. Dimensions and process parameters of these platinum microheaters were as described in a previous work.[23] Although contacting with the copper vias already takes place in this process step due to sputtering under an angle, an additional aluminum deposition in the contact area (layer thickness 700 nm) improves the electrical contact (Figure 2 e). Before synthesizing the hydrogel layers, another polyimide layer was laminated over the previously created microheater array to provide electrical insulation and a barrier from the aqueous hydrogel environment (see Figure 2 f).

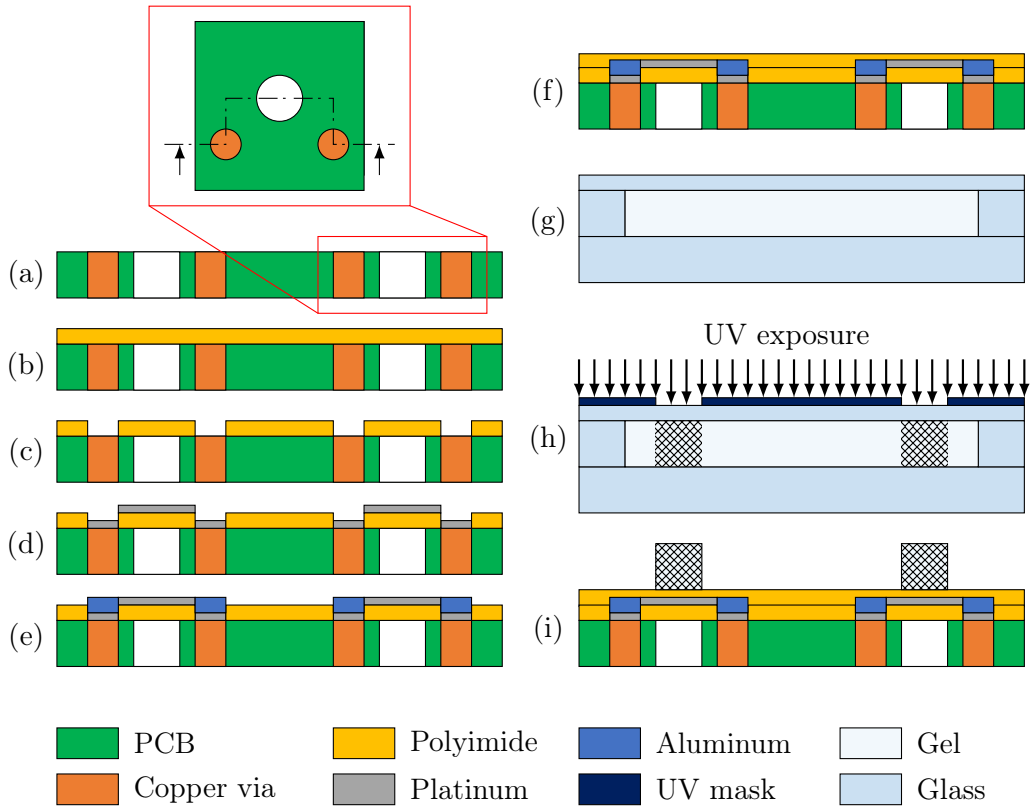


Figure 2: Illustration of the process steps for fabricating a hydrogel-based microactuator platform. (a) to (b) a polyimide layer is laminated onto the PCB, which has holes and copper vias. (c) The polyimide in the area of the copper vias is removed, (d) platinum heater meanders are deposited and (e) contacted with the vias. (f) sealing of the microheaters with a polyimide layer. (g) Pregel application, (h) UV patterning of the temperatur-sensitive hydrogel on a glass substrate and (f) alignment of the hydrogel actuators with the microheaters.

## 2.2 Hydrogel actuator array

The composition of the *net*-PNiPAAm hydrogel[24] as well as the pillar fabrication technique[25] are based on previous works. The initiator system was changed to photoinitiation using the photoinitiator Lithium phenyl-2,4,6-trimethylbenzoylphosphinate (LAP). *N*-isopropylacrylamide (NiPAAm), *N,N'*-methylenebis(acrylamide) (MBA) and LAP were bought from Sigma-Aldrich (USA) and used as received. For the pregel solution 250 mg NiPAAm, 0.825 mL MBA (used as a stock solution with 20 mg $mL^{-1}$) and 0.184 mL LAP (used as a stock solution with 40 mg $mL^{-1}$) were dissolved in 0.491 mL deionized water. The addition of LAP and subsequent processing was performed under low UV illumination. The solution was degassed with Argon for 10 min and subsequently cooled in an ice water bath.

An acrylic spacer of thickness 1 mm was placed on a microscope glass slide covered with a UV and temperature resistant tape (Crystal clear, Gorilla Glue Inc.), see Figure 2 g. The acrylic spacer has a recess in the area of the

microheater structures, which was filled with the pregel solution and subsequently closed with a thin glass slide (18 mm x 18 mm, thickness 100 µm). The glass slide was previously stored in an Argon atmosphere to decrease oxygen presence during the radical polymerization, which is known to promote the adherence of PNiPAAm-based hydrogels on glass.[26] A UV mask (Fineline Imaging, Inc.) with circular openings of diameter 750 µm matching the pattern of the microheaters was placed on top of the glass. Clamps and Parafilm were used to fix and seal the bottom glass slide, the spacer, the thin top glass slide and the UV mask.

Still being cooled with ice, the polymerization was initiated with a UV lamp (3.46 mW $cm^{-2}$), see Figure 2 h. In a second experiment, the pregel solution and assembly was not cooled but crosslinked at room temperature (23 °C) instead. After 20 s the UV lamp was turned off, the assembly was taken apart and the excess pregel solution was removed by rinsing with deionized (DI) water. The remaining hydrogel pillars adhere to the thin glass slide and are kept wet from then on to avoid cracks and shear stress due to drying. They were submerged in water and the water was changed three times to rinse out unreacted residues. The glass slide is flipped and clamped to the microheater array as shown in Figure 2 i. Although direct attachment of the hydrogel pillars to the polyimide surface via polyimide surface functionalization as used for other hydrogels in a previous work would be preferred,[27] this attachment procedure did not succeed for PNiPAAm-based hydrogels in this work. Since PNiPAAm-based hydrogels adhere sufficiently well to glass substrates,[26] the approach shown here with the thin glass slide was chosen to demonstrate a proof-of-principle for a hydrogel actuator array on a PCB-based micro-heater array.

### 2.3 Free swelling experiments

Circular discs of the hydrogel were prepared using two acrylic slides with an acrylic spacer (1 mm thick and a circular cutout of 15 mm) in between. The synthesis was carried out as described in the previous section. The hydrogel discs were placed in vessels and washed by changing the DI water for three times as well as conditioned by applying temperature cycles between room temperature and 45 °C. Subsequently, free swelling experiments were carried out by immersing the vessels in a thermostatic bath at temperatures of 20 °C, 25 °C, 30 °C, 35 °C, 40 °C and 45 °C. After the samples were kept at this temperature for 12 h, the samples' diameters were captured with a camera and determined with the software ImageJ to asses the temperature-dependent swelling behavior.

### 2.4 Selective hydrogel actuation

Using a resistance measurement as shown in a previous paper, the functional microheaters were determined. Typically, approx. 90% of the microheaters in a 10x10 array are functional.[?,23] These microheaters were contacted from the backside of the PCB via the copper vias. For actuation, a voltage was applied to individual microheaters so that they operated at a constant power of 150 mW. Actuating experiments were carried out in an aqueous environment. An acrylic frame of 2.5 mm height was used to create a reservoir above the area of the microheater array. This reservoir was completely filled with water and closed with an acryl plate to reduce optical artifacts of the water surface. The response of the hydrogel was recorded via a microscope (Keyence VHX-5000).

## 3. MODELING AND SIMULATION WITH THE TEMPERATURE EXPANSION MODEL

The design of a micromanipulation platform based on the microheater array and active hydrogels requires the consideration of the heat conduction and the actuation behavior. In the current section, the multi-field description of the involved physical fields is described in section 3.1. The actuation behavior of hydrogels is modeled with the Temperature-Expansion-Model in section 3.2.

### 3.1 Multi-field description for the setup

When a single heater in the heater array is activated, the temperature difference leads to (i) a heat flow through the polyimide and glass layers to the hydrogel pillars, see Figure 3. However, at the same time, the hydrogel is also in contact with the surrounding water and the swelling/deswelling (ii) mass transport leads to an enthalpy transfer (material-inherent heat transfer). Additionally, the (iii) mechanic boundary conditions impose restrictions to the local swelling and subsequently to mass transfer.

Therefore, due to the setup, the result of the local swelling is complex and three-dimensional. This requires either (A) the 3D space- and time-resolved solution of the coupled mass- and heat-transfer equations as well as mechanical field equations or (B) strong assumptions towards the equilibrium conditions that are already reached.

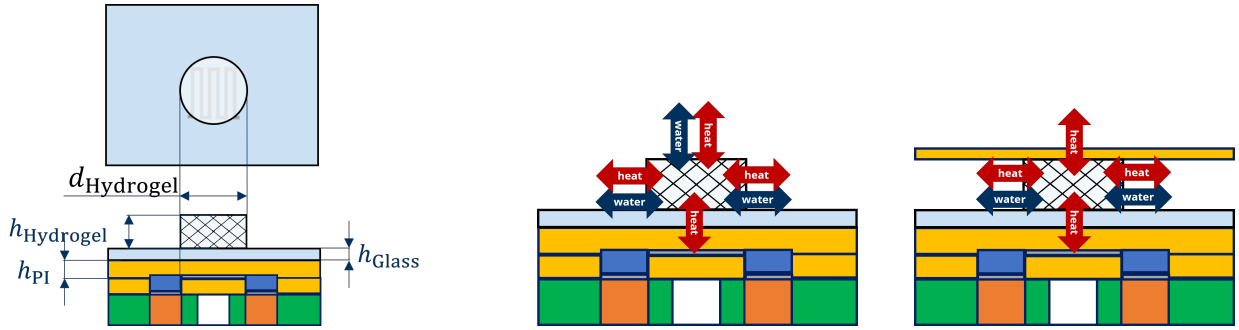


(a) Schematic view of the layers. (b) Free cylinders. (c) Cylinders with mirror base.

Figure 3: For the approach (A), i.e., the multi-field modeling of the setup, the different layers (a) with their properties (heat conductivity, heat capacity, heights) have to be described. Based on these properties, the stimulus and water transfer directions and the mechanical conditions at the boundaries can be defined. These are the boundary conditions for the involved fields in the three-dimensional coupled multi-field description of the micromanipulator platform's actuation for (b) the free pillars and (c) with a mounted mirror.

For the (A) space- and time-resolved modeling, a continuum multi-field approach based on the Theory of Porous Media can be applied. This includes the momentum balances, kinematics and material behavior. The material is homogenized based on the Theory of Mixtures and the concept of volume fractions.[28,29] An alternative approach is based on poromechanics.[30]

The main focus of the present work is on the fabrication process and proof-of-concept. Therefore, the simplified approach (B) is applied and the (A) complex 3D approach will be part of our future works. For the (B) simplified approach we assume an equilibrium where

- the temperature of the platinum meanders and the surrounding PCB material is the same. This is also supported by thermal imaging results.[23]
- the immediate surrounding water of the hydrogel cylinder is of the same temperature as inside the cylinder. Thus, no enthalpy transport occurs with swelling and deswelling. This assumption is justified when the water reservoir is (i) very small (low total heat capacity) and thermally isolated or (ii) no stirring/mixing occurs (leading to a thermal skin effect).[31]
- the cylinder has reached a constant temperature
- the swelling/deswelling (water transport) process is completed.

When these assumptions hold, the local swelling is only dependent on the temperature and the mechanical constraints and can be modeled based on the Temperature-Expansion-Model, which is described in the following section.

### 3.2 Temperature Expansion Model for actuation

When the assumptions for the simplified description described in the previous section hold, the swelling behavior of the hydrogel cylinders can be described with the Temperature-Expansion-Model.[32,33] The basic idea is the analogy of the phenomenological descriptions of thermal expansion in metals and isotropic swelling of hydrogels (despite the different physical background).

In equilibrium, the state of a hydrogel body can be described with the following equations:

$$\text{Balance laws} \qquad \sigma_{kl,k} + f_l = 0 \qquad \sigma_{kl} = \sigma_{lk} \tag{1}$$

$$\text{Kinematics} \qquad \varepsilon^{\mathrm{H}}_{kl} = \frac{1}{2}\ln(B_{kl}) \tag{2}$$

$$\text{Material behavior} \qquad \sigma_{kl} = E_{klmn}\left(\varepsilon^{\mathrm{H}}_{mn} - \beta(F^{\mathrm{Stimulus}})\,\delta_{mn}\,\Delta F^{\mathrm{Stimulus}}\right) \tag{3}$$

Here, $\sigma_{kl}$ denotes the stress tensor, $f_l$ are volume loads and $\varepsilon^{\mathrm{H}}_{kl}$ is the nonlinear HENCKY strain which is based on the Cauchy deformation tensor $B_{kl}$. The elastic constants (YOUNG's modulus and POISSON ratio) can be found in the elasticity tensor $E_{klmn}$. The isotropic expansion is included with the isotropic stimulus expansion coefficient $\beta$ and the stimulus ratio $\Delta F^{\mathrm{Stimulus}}$. Partial derivatives with respect to $x_k \in [x, y, z]$ or $[x_1, x_2, x_3]$ are denoted by $()_{,k}$, EINSTEIN's summation convention holds and $\delta_{kl}$ is the KRONECKER delta. The model can also be extended to include additional stimuli for multisensitive hydrogels.[34]

Simulation results for hydrogel pillars are presented in section 4.3. There, also the normalization procedure that is used to bring the experimental data into the commercial Finite-Element tool is shown.

## 4. RESULTS AND DISCUSSION

In the current section, the results of free swelling (section 4.1) and of actuated pillars (section 4.2) is presented. This is followed by the simulation results (section 4.3).

### 4.1 Free swelling results of the hydrogel material

The results of the free swelling measurement are shown in Figure 4. The volume phase transition behavior typical for PNiPAAm hydrogels can be seen. If the synthesis is carried out under cooled conditions, transparent hydrogels are formed, which show an overall larger volume response than in the case of room-temperature synthesis. The transparency changes to a whitish opacity at higher temperatures and shrinking. The hydrogel samples from the non-cooled synthesis, on the other hand, are opaque even in the swollen state due to permanent phase separation.[22] The swelling measurement data shown here were collected for simulation with the temperature expansion model and used in there. The unloaded reference swelling state is considered to be the swelling degree that is present immediately upon synthesis. This reference state corresponds exactly to the diameter of the mold used.

### 4.2 Experimental results for the actuation capabilities

A fabricated microheater array with a close-up view of a single microheater is shown in Figure 5 a. It contains 100 microheaters on an area of 15 x 15 $\mathrm{mm}^2$. Figure 5 b shows the hydrogel actuators fabricated on the glass slide under cooled conditions. The image is taken under non-aqueous conditions, resulting in a slightly conical structure due to partial drying. A slightly conical structure may also be caused by the UV exposure setup, which can lead to inhomogeneous polymerization in the opening area of the mask. Figure 5 c shows a top-view and close-up area of the microheater array equipped with hydrogel actuators immersed in water.

Figure 6 shows an example of three adjacent hydrogel actuators that are controlled alternately. The hydrogel's activation is clearly visible due to the additional change from transparent appearance to whitish opacity that accompanies the phase transition. It can be stated that there is no significant crosstalk between hydrogel actuators. Even with longer actuation of 1 min, the neighboring non-addressed actuator retains its shape and transparency. After several heating cycles, shearing from the polyimide surface was observed for some hydrogel actuators, possibly indicating that the hydrogel actuators adherence to the glas surface is strong enough.

### 4.3 Simulation results of the two setups

The normalization procedure (according to the steps described in section 3.2) for the experimental free swelling data of the transparent samples (see Figure 3a) leads to the HENCKY strain curve and nonlinear expansion coefficient curves according to Figure 7. The $\beta$-curve is the base for the simulations in the Finite-Element software Abaqus. For the mechanical properties of the hydrogel, the behavior of *net*-PNiPAAm was taken from literature.[20,35]

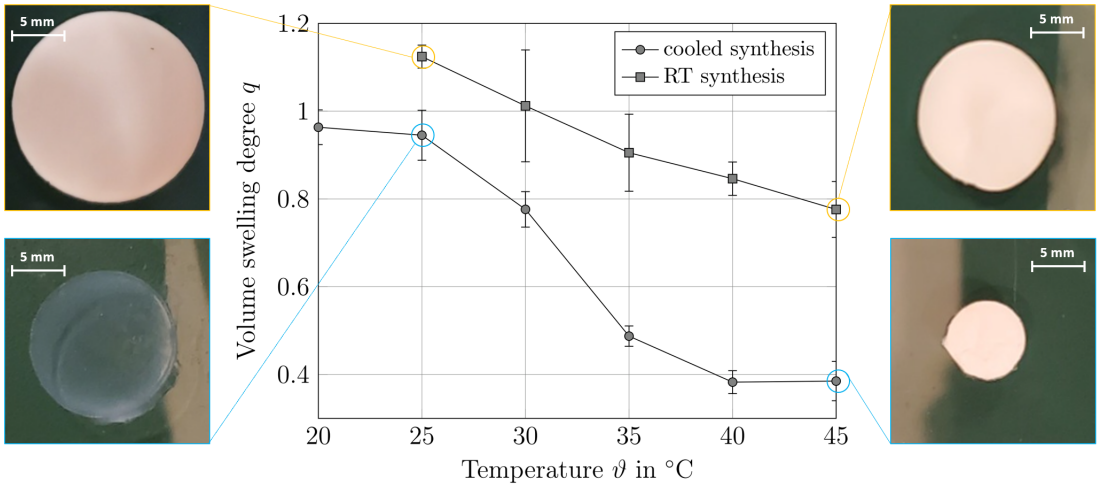


Figure 4: Free swelling of hydrogel discs ($n = 4$, confidence interval of 95%) that were prepared by a cooled synthesis and a synthesis at room temperature. Please note that in the following considerations and derivations like the expansion coefficient (Figure 7) were only based on the transparent hydrogels from the cooled synthesis.

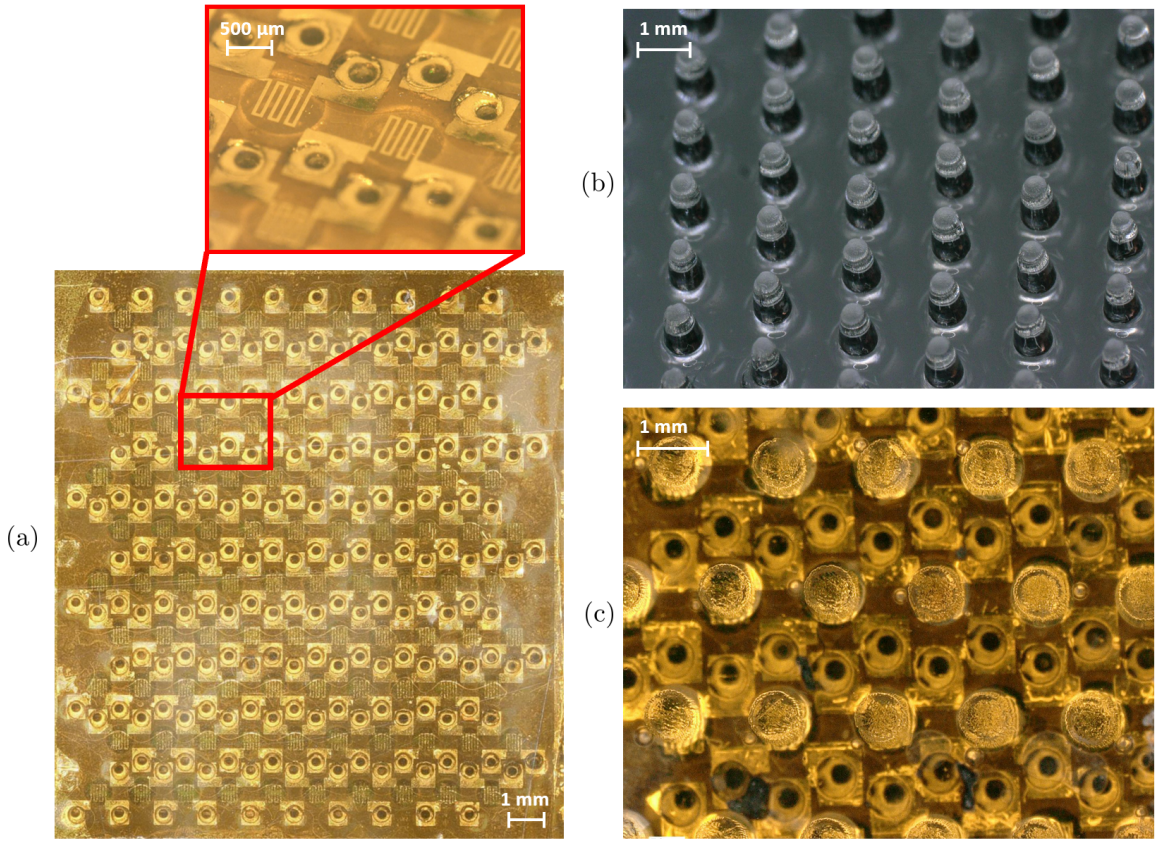


Figure 5: Images of (a) the polyimide encapsulated 10x10 micro heater array, (b) the hydrogel actuators on the glass slide (actuators partly dried) and (c) the micro-actuator platform after hydrogel actuator alignment on the microheaters (actuators immersed in water).

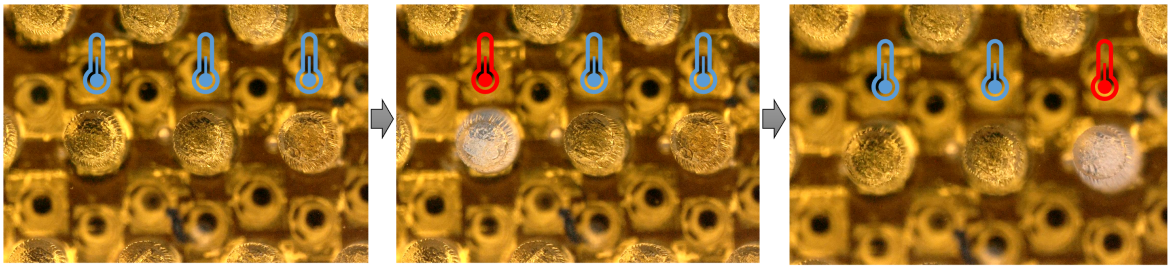

t=0 s t=15 s t=30 s

Figure 6: Three adjacent hydrogel actuators are shown in an overhead view in an aqueous environment. The left and the right hydrogel actuator are successively excited by a heat current supply from the microheaters. The change in transparency to a whitish haze of the hydrogel indicates a phase transition.

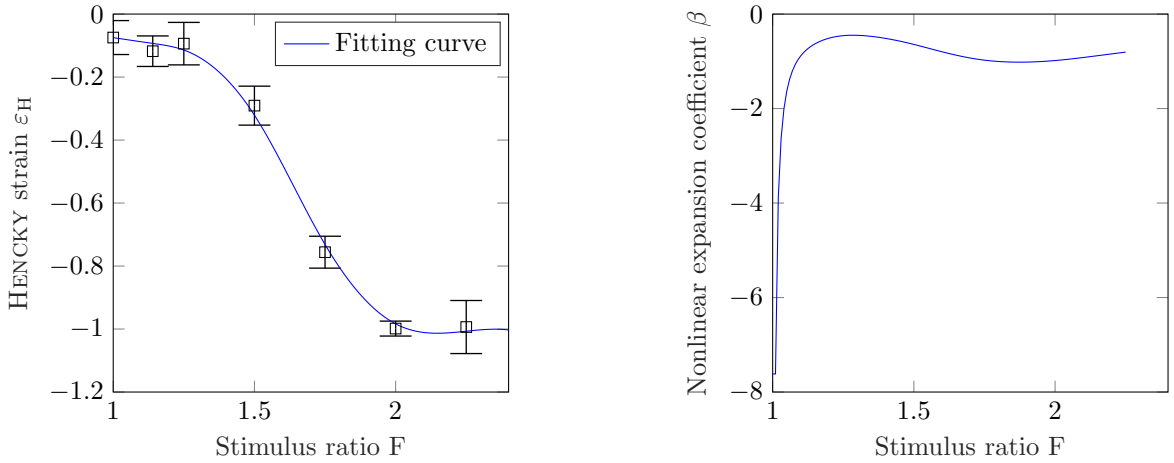


(a) Hencky curve for the derivation of the $\beta$-curve. (b) Expansion coefficient $\beta$ for implementation.

Figure 7: Nonlinear Hencky strain over stimulus ratio and nonlinear expansion coefficient based on the transparent samples in Figure 3a.

Numerical simulations of the microheater array setup with hydrogel dots and with a rigid top layer (Kapton (R) polyimide on which the mirror element can be attached, see Figure 1) were performed. The elastic properties of the top layer ($E_{\text{Kapton}} = 2.28\,\text{GPa}$) and the bottom glass slide ($E_{\text{Borosilicate Glass}} = 60\,\text{GPa}$) generate a stiffness ratio that leads to *constrained swelling* according to the classification in our previous work.[36] The Finite-Element simulations in Abaqus were based on the equilibrium assumptions described in section 3.1 and on the Temperature-Expansion-Model described in section 3.2.

In Figure 8, the results for the activation of a single heater are depicted. Due to the assumptions described above, the local temperature in one pillar does not impact the surrounding ones, which was also observed experimentally, see Figure 6. We therefore simulate only the actuation of one cylinder, see Figure 8a.

Due to the constrained swelling regime, the mechanical stress is concentrated at the contact point, see Figure 8a. This can lead to a shearing-off of the pillars from the substrate, which was also observed in the experiments (section 4.2). From the magnitude of the displacement (Figure 8b), it can be seen that only a small diameter change happens. However, due to the cyclindrical shape, the displacement in height-direction is suitable for tilting a mirror element.

The simulation results of the tilting of mirror elements with the micro-heater array are depicted in Figure 9.

From the simulation results, we expect that even though the hydrogel is not itself capable of deforming the top layer, we can still achieve a tilting of the mirror structure. The combined actuation of multiple pillars can lead to a change of tilting direction. Higher tilting angles can be achieved by using higher pillars, because the same swelling strain leads to a higher swelling displacement.

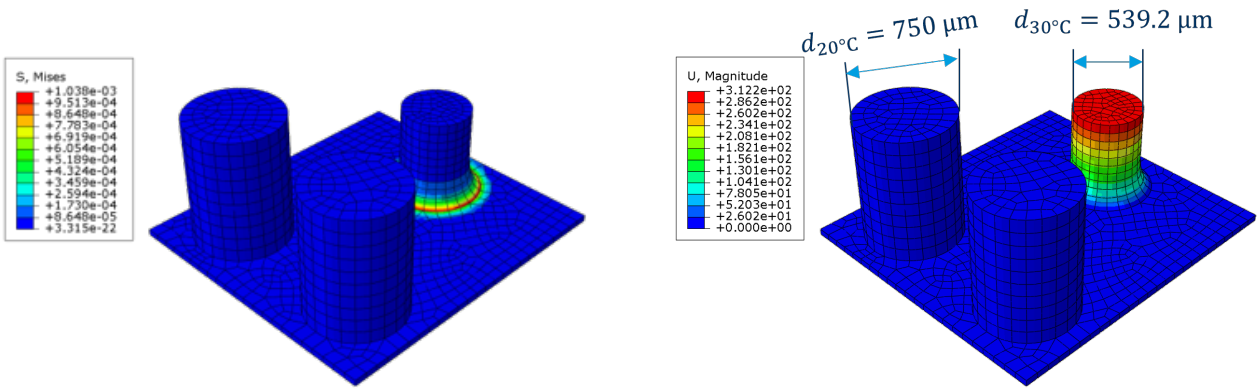


(a) Magnitude of Mises stress in the pillar.

(b) Magnitude of displacement in the pillar.

Figure 8: Swelling of one pillar on the array. The simulations were performed in Abaqus with 2709 quadratic elements of the type C3D20H. The bottom part is fixed and a temperature difference of 10 °C was applied. Due to the fixture at the bottom, the cylinder diameter cannot change freely. However, even though only a small diameter change can be observed, there is a notable height change due to the properties of cylinder shapes under isotropic swelling conditions.

To achieve arbitrary tilting directions, a precise actuation of every pillar is necessary. Since the micro-heater meanders are constant heat flow sources, an adequate cooling to stabilize the temperature is necessary. This will be part of our future studies with this system.

## 5. CONCLUSION AND OUTLOOK

In this work we showed a proof-of-principle hydrogel-based actuator platform which is intended to affect surfaces, while using a printed circuit board (PCB) as the wiring carrier and membrane-suspended microheaters for the local excitation of the hydrogel actuators. We succeeded in fabricating a 10x10 array of individually addressable hydrogel actuators. These 100 actuators span an area of 15 mm x 15 mm, resulting in an actuator density of approx. 44 $cm^{-2}$. Due to the membrane suspension, the microheaters in our setup have a comparatively low power consumption of 150 mW. A major advantage of this actuator principle is its high energy density and that the hydrogel actuator is functional in an aqueous environment unlike various other actuator principles. It may therefore be appropriate for applications such as moisture-retaining lenses. A model of such a hydrogel-based actuator array was shown. Finite-Element simulations based on the Temperature-Expansion Model show the actuation potential of these microactuators using the example of tiltable surfaces. In the current setup and with the *net*-PNiPAAm hydrogel used as the active material, inclination angles of up to 15° are theoretically possible. However, higher hydrogel pillars lead to a larger displacement for the same swelling actuation and thus to a higher tilting capacity. The advantage of using triangular sub-surfaces, each resting on three pillars, is that because of this division, openings already exist in the surface that are favorable for water exchange between the top and bottom surfaces. The extension of the experimental setup to include such cover surfaces is subject of further research. This also includes the fixed definition of a temperature operating point by e.g. closed-loop control operation of each heater or water cooling to stabilize defined intermediate swelling states. This can lead to the construction of fish-scale-like adaptable skins for underwater surfaces, that adapt to the local fluidic field conditions.

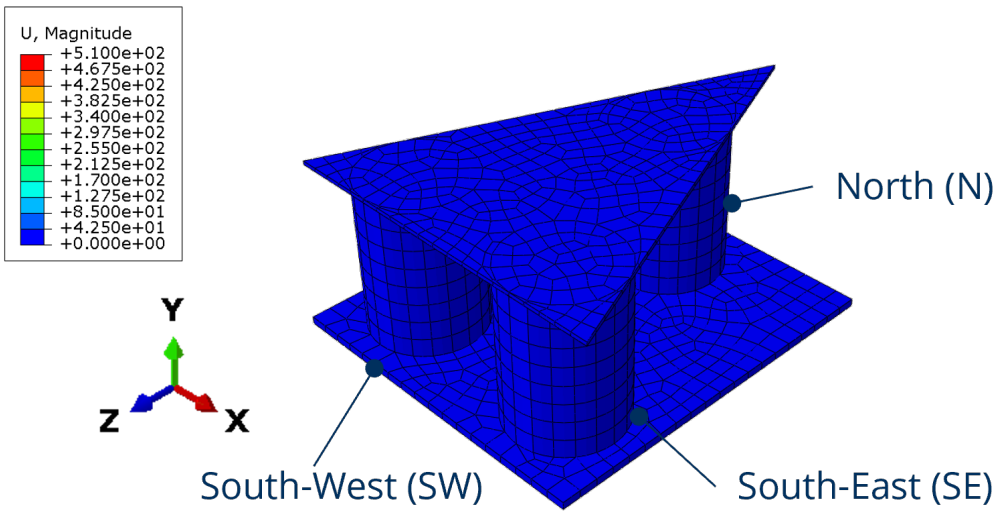


(a) A triangle with the material property of polyimide according to section 2 is brought to the top of the hydrogel pillars. The triangle is designed such that it is tangent to the tops of the cylinders. The colorbar is valid for all plots (b)-(d).

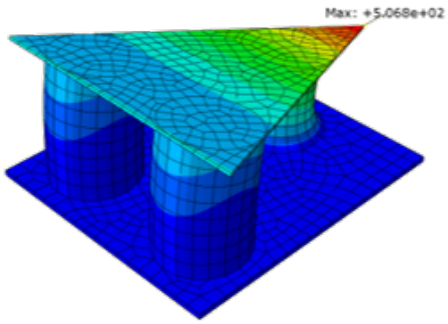


(b) Actuated pillar N, total angle: 11.6°.

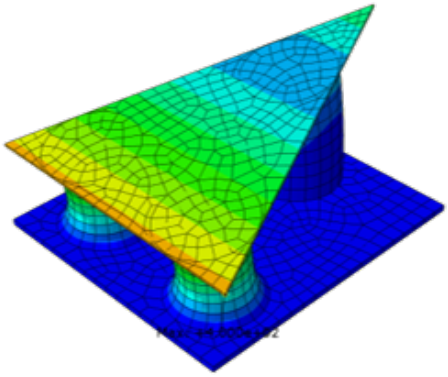

(c) Actuated pillars SE and SW, total angle: 11.7°.

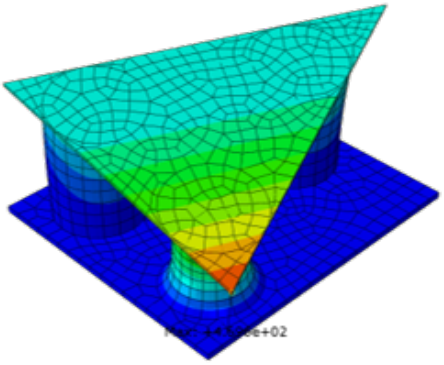

(d) Actuated pillar SE, total angle: 14.5°.

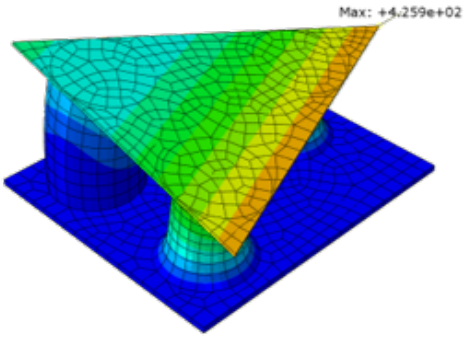


(e) Actuated pillars SE and N, total angle: 15.0°.

Figure 9: Swelling of a pillars on the array with a quasi-rigid polyimide top layer. The total angle is between the titled top plane and the bottom plane. A total of 1922 hybrid quadratic elements C3D20H were used for the simulation.

## ACKNOWLEDGMENTS

This work was performed in part at the Utah Nanofab sponsored by the College of Engineering, Office of the Vice President for Research, and the Utah Science Technology and Research (USTAR) initiative of the State of Utah. The authors appreciate the support of the staff and facilities that made this work possible.
The development of the employed microheater array fabrication process was originally supported by the United States Department of Energy under award number DE-SC0017168 awarded to Particle Flux Analytics Inc. The authors would like to thank Allan Reaburn and his colleagues at Particle Flux Analytics for their contributions.
Adrian Ehrenhofer thanks for the financial funding of the Dresden Center for Intelligent Materials (DCIM) by the Free State of Saxony (Germany) and TU Dresden.
Simon Binder acknowledges funding by the Deutsche Forschungsgemeinschaft (DFG, German Research Foundation) – 459675326.

According to the CrediT system, the authors contributed to this publication as follows:
SB: Fabrication and experimental part conceptualization, data curation, formal analysis, investigation, methodology, validation, visualization, writing - original draft, funding acquisition;
AE: Modeling and simulation part conceptualization, data curation, formal analysis, investigation, methodology, validation, visualization, writing - original draft, funding acquisition;
TA: Conceptualization, experiments, data curation, formal analysis, review & editing;
CR: Writing – review & editing, resources, supervision, project administration;
FS: Writing – review & editing, resources, supervision, funding acquisition, project administration;
TW: Writing – review & editing, resources, supervision, funding acquisition, project administration.

## CONFLICT OF INTEREST

The authors declare the following competing financial interests that are managed through the University of Utah conflict of interest management: F. Solzbacher declares a financial interest in Sentiomed, Inc. and Blackrock Microsystems/Blackrock Neuromed.

The fundamental intellectual property of the microheater array fabrication process is protected by the following patent application filed by the University of Utah Research Foundation: Micro-Electromechanical Systems Including Printed Circuit Boards and Pre-Fabricated Polymer Films, WO 2020061356A2 with M. Leber, F. Solzbacher and B. Baker listed as inventors. This Intellectual property is exclusively licensed to Particle Flux Analytics Inc.

## REFERENCES

[1] Tortschanoff, A., Lenzhofer, M., Frank, A., Wildenhain, M., Sandner, T., Schenk, H., Scherf, W., and Kenda, A., "Position encoding and phase control of resonant moems mirrors," *Sensors and Actuators A: Physical* **162**(2), 235–240 (2010).

[2] Zimmer, F., Grueger, H., Heberer, A., Sandner, T., Wolter, A., and Schenk, H., "Scanning micro-mirrors: From bar-code scanning to spectroscopy," in [*Optical Scanning 2005*], Sagan, S. F. and Marshall, G. F., eds., **5873**, 84–94, International Society for Optics and Photonics, SPIE (2005).

[3] Wallrabe, U., "Axicons et al. - Highly aspherical adaptive optical elements for the life sciences," in [*Transducers 2015 - 18$^{th}$ International Conference on Solid-State Sensors, Actuators and Microsystems*], 251–256 (2015).

[4] Richter, A. and Paschew, G., "Optoelectrothermic control of highly integrated polymer-based mems applied in an artificial skin," *Advanced Materials* **21**(9), 979–983 (2009).

[5] Vidal-Verdu, F. and Hafez, M., "Graphical tactile displays for visually-impaired people," *IEEE Transactions on Neural Systems and Rehabilitation Engineering* **15**(1), 119–130 (2007).

[6] Cho, H.-C., Kim, B.-S., Park, J.-J., and Song, J.-B., "Development of a braille display using piezoelectric linear motors," in [*2006 SICE-ICASE International Joint Conference*], 1917–1921, IEEE (2006).

[7] Balabozov, I., Yatchev, I., and Hinov, K., "Computer modeling and experimental verification of dynamic characteristics of permanent magnet linear actuator for braille screen," in [*2014 International Conference on Applied and Theoretical Electricity*], 1–4, IEEE (2014).

[8] Yobas, L., Durand, D. M., Skebe, G. G., Lisy, F. J., and Huff, M. A., "A novel integrable microvalve for refreshable braille display system," *Journal of Microelectromechanical Systems* **12**(3), 252–263 (2003).

[9] Choi, H. R., Lee, S., Jung, K. M., Koo, J. C., Lee, S., Choi, H., Jeon, J. W., and Nam, J.-D., "Tactile display as a braille display for the visually disabled," in [*2004 IEEE International Conference on Intelligent Robots and Systems (IROS)*], **2**, 1985–1990, IEEE (2004).

[10] Qu, X., Ma, X., Shi, B., Li, H., Zheng, L., Wang, C., Liu, Z., Fan, Y., Chen, X., and Li, Z., "Refreshable braille display system based on triboelectric nanogenerator and dielectric elastomer," *Advanced Functional Materials* **31**(5), 2006612 (2021).

[11] Ren, K., Liu, S., Lin, M., Wang, Y., and Zhang, Q., "A compact electroactive polymer actuator suitable for refreshable braille display," *Sensors and Actuators A: Physical* **143**(2), 335–342 (2008).

[12] Haga, Y., Makishi, W., Iwami, K., Totsu, K., Nakamura, K., and Esashi, M., "Dynamic braille display using SMA coil actuator and magnetic latch," *Sensors and Actuators A: Physical* **119**(2), 316–322 (2005).

[13] Kwon, H.-J., Lee, S. W., and Lee, S. S., "Braille dot display module with a PDMS membrane driven by a thermopneumatic actuator," *Sensors and Actuators A: Physical* **154**(2), 238–246 (2009).

[14] Besse, N., Rosset, S., Zarate, J. J., and Shea, H., "Flexible active skin: large reconfigurable arrays of individually addressed shape memory polymer actuators," *Advanced Materials Technologies* **2**(10), 1700102 (2017).

[15] Heikenfeld, J., Smith, N., Dhindsa, M., Zhou, K., Kilaru, M., Hou, L., Zhang, J., Kreit, E., and Raj, B., "Recent progress in arrayed electrowetting optics," *Optics & Photonics News* **20**(1), 20–26 (2009).

[16] Jeong, K.-H., Liu, G. L., Chronis, N., and Lee, L. P., "Tunable microdoublet lens array," *Optics Express* **12**(11), 2494–2500 (2004).

[17] Greiner, R., Allerdissen, M., Voigt, A., and Richter, A., "Fluidic microchemomechanical integrated circuits processing chemical information," *Lab on a Chip* **12**(23), 5034–5044 (2012).

[18] Beebe, D. J., Moore, J. S., Bauer, J. M., Yu, Q., Liu, R. H., Devadoss, C., and Jo, B.-H., "Functional hydrogel structures for autonomous flow control inside microfluidic channels," *Nature* **404**(6778), 588–590 (2000).

[19] Richter, A., Klatt, S., Paschew, G., and Klenke, C., "Micropumps operated by swelling and shrinking of temperature-sensitive hydrogels," *Lab Chip* **9**, 613–618 (2009).

[20] Ehrenhofer, A., Hahn, M., Hofmann, M., and Wallmersperger, T., "Mechanical behavior and pore integration density optimization of switchable hydrogel composite membranes," *Journal of Intelligent Material Systems and Structures* **31(3)**, 425–435 (2020).

[21] Binder, S. and Gerlach, G., "Performance of force-compensated chemical sensors based on bisensitive hydrogels," *Sensors and Actuators B: Chemical* **342**, 129420 (2021).

[22] Gehrke, S. H., "Synthesis, equilibrium swelling, kinetics, permeability and applications of environmentally responsive gels," in [*Responsive Gels: Volume Transitions II*], Dušek, K., ed., 81–144, Springer, Berlin, Heidelberg (1993).

[23] Ahmad, T., Binder, S., Leber, M., Garrett, T. J., Reiche, C. F., and Solzbacher, F., "Fabrication of polymer membrane-suspended microstructures on printed circuit boards," *Journal of Microelectromechanical Systems* (2022, accepted).

[24] Franke, D., Binder, S., and Gerlach, G., "Performance of fast-responsive, porous crosslinked poly(N-isopropylacrylamide) in a piezoresistive microsensor," *IEEE Sensors Letters* **PP**, 1–1 (11 2017).

[25] Farhoudi, N., Magda, J. J., Solzbacher, F., and Reiche, C. F., "Fabrication process for free-standing smart hydrogel pillars for sensing applications," in [*Proceedings of the 2020 IEEE Sensors Conference*], 20212246 (2020).

[26] Beck, A., Obst, F., Busek, M., Grünzner, S., Mehner, P. J., Paschew, G., Appelhans, D., Voit, B., and Richter, A., "Hydrogel patterns in microfluidic devices by Do-It-Yourself UV-photolithography suitable for very large-scale integration," *Micromachines* **11**(5), 479 (2020).

[27] Kairy, P. D., Farhoudi, N., Binder, S., Magda, J. J., Kuck, K., Solzbacher, F., and Reiche, C. F., "Catheter-mounted smart hydrogel ultrasound resonators for intravenous analyte monitoring," in [*43rd Annual International Conference of the IEEE Engineering in Medicine Biology Society (EMBC)*], 7476–7479 (2021).

[28] Ehlers, W., "Grundlegende Konzepte in der Theorie Poröser Medien," *Technische Mechanik 16* **16**(16), 63–76 (1996).

[29] Leichsenring, P. and Wallmersperger, T., "Modelling and simulation of the chemically induced swelling behavior of anionic polyelectrolyte gels by applying the theory of porous media," *Smart Materials and Structures* **26(3)**, 035007 (2017).

[30] Coussy, O., "Problems of poroelasticity," in [*Poromechanics*], 113–150, John Wiley & Sons (2004).

[31] Yoshida, R., Sakai, K., Okano, T., Sakurai, Y., Bae, Y. H., and Kim, S. W., "Surface-modulated skin layers of thermal responsive hydrogels as on-off switches: I. drug release," *Journal of Biomaterials Science, Polymer Edition* **3**(2), 155–162 (1992).

[32] Ehrenhofer, A., Bingel, G., Paschew, G., Tietze, M., Schröder, R., Richter, A., and Wallmersperger, T., "Permeation control in hydrogel-layered patterned pet membranes with defined switchable pore geometry - experiments and numerical simulation," *Sensors and Actuators B: Chemical* **232**, 499–505 (2016).

[33] Ehrenhofer, A., Elstner, M., and Wallmersperger, T., "Normalization of hydrogel swelling behavior for sensoric and actuatoric applications," *Sensors and Actuators B: Chemical* **255**(Part 2), 1343 – 1353 (2018).

[34] Ehrenhofer, A., Binder, S., Gerlach, G., and Wallmersperger, T., "Multisensitive swelling of hydrogels for sensor and actuator design," *Advanced Engineering Materials* **22**(7), 2000004 (2020).

[35] Seuss, M., Schmolke, W., Drechsler, A., Fery, A., and Seiffert, S., "Core–shell microgels with switchable elasticity at constant interfacial interaction," *ACS applied materials & interfaces* **8**(25), 16317–16327 (2016).

[36] Ehrenhofer, A. and Wallmersperger, T., "Shell-forming stimulus-active hydrogel composite membranes: Concept and modeling," *Micromachines* **11(6)**, 541 (2020).